Front. Chem. China 2007, 2(3): 278–282
DOI 10.1007/s11458-007-0050-4

RESEARCH ARTICLE

LONG Mingce, CAI Weimin, CHEN Heng, XU Jun

Preparation, characterization and photocatalytic activity of visible light driven chlorine-doped TiO_2

Abstract A novel chlorine-doped titanium dioxide catalyst with visible light response was prepared by hydrolysis of tetrabutyl titanate in hydrochloric acid. The catalyst samples were characterized by X-ray diffraction (XRD), transmission electron microscopy (TEM), X-ray photoelectron spectroscopy (XPS), and ultraviolet-visible diffuse reflectance spectroscopy (UV-Vis DRS). Results showed that the doped element of Cl lowered the temperatures of phase transformation of TiO_2 from amorphous to anatase and from anatase to rutile. The absorption edge of chlorine-doped TiO_2 calcined at 300°C shifted to visible light region. X-ray photoelectron spectroscopy results proved that chlorine existed in the TiO_2 crystal lattice as anion. The photocatalytic degradation of phenol showed that under visible light ($\lambda > 400$ nm) irradiation, the chlorine-doped TiO_2 calcined at 300°C displayed the best performance, the degradation ratio of phenol was 42.5% after 120 min.

Keywords titanium dioxide, chlorine doping, visible light, photocatalysis, phenol

1 Introduction

In 1976, Carey and his coworkers first reported the degradation of the organic pollutant polychlorinated bipheny by TiO_2 photocatalysis [1]. Since then, the studies on degradation and mineralization of persistent toxic organic pollutants by semiconductor photocatalysis have always been focused. Because nearly all organic pollutants can be photocatalytically degraded, and it is possible to remove the persistent toxic organic pollutants by using only atmospheric oxygen and solar energy, photocatalysis is promising as a green environmental control technology [2]. Due to its advantages, such as high efficiency, stability and economy, TiO_2 has been investigated extensively in photocatalytic reaction. However, its band gap is too wide ($E_g = 3.2$ eV), which can only respond to the ultraviolet light with the wavelength below 387 nm. Because more than 45% energy in solar spectrum is visible light, the excitation wavelength becomes the bottleneck of the photocatalytic application of TiO_2.

By doping certain elements into the crystal of TiO_2, and introducing impurity or defect levels into the band gap, the energy for electron excitation in TiO_2 can be decreased and its absorption can be extended into visible light range. In the earlier researches, much attention has been paid on metal doping. However, the external metal ion can form recombination centers, resulting in decreasing efficiency, and an unacceptable stability of metal-doped TiO_2 [3]. In 2001, Asahi first reported N-doped TiO_2 with good performance under visible light irradiation [3], and nonmetal doping of TiO_2 immediately stirred great interests. N [4,5], C [6,7], S [8,9], I [10,11] and other nonmetal elements used in doping TiO_2 all exhibited certain visible light photocatalytic responses. And TiO_2, codoped with metal and nonmetal elements, showed even better activity in visible light [12–14]. In this paper, hydrolyzation of tetrabutyl titanate in hydrochloric acid chlorine-doped TiO_2 nanoparticles has been prepared, and the novel photocatalyst exhibits good photocatalytic activity under visible light irradiation.

2 Experiments

2.1 Preparation of photocatalysts

Chlorine-doped TiO_2 nanoparticles have been prepared as follows: tetrabutyl titanate was added into hydrochloride acid solution ($V/V = 1{:}1$) dropwise and stirred for half an hour to hydrolyze completely. The formed white precipitate was the precursor, which was dried in an oven at 120°C, then ground to dried gel powder. The powder was calcined at different temperatures for 2 h in a programmed oven with a calefactive velocity 5°C/min.

Translated from *Chinese Journal of Catalysis*, 2006, 27(10): 890–894
[译自: 催化学报]

LONG Mingce, CAI Weimin (✉), CHEN Heng, XU Jun
School of Environmental Science and Engineering, Shanghai Jiaotong University, Shanghai 200240, China
E-mail: wmcai@sjtu.edu.cn

2.2 Characterization of photocatalysts

The X-ray powder patterns of the photocatalysts were obtained on a Bruker D8 ADVANCE polycrystalline diffractometer, with the voltage 40 kV and current 40 mA. The size and shape of the particles were observed using a transmission electron microscope (TEM, JEM-2010 JEOL). Samples were sonicated in ethanol suspension and dropped onto a copper net for observation. The specific surface area of the samples was determined using a Micromeritrics ASAP 2010 nitrogen adsorption apparatus and by Brunauer-Emmett-Teller (BET) method with 8 point isothermal adsorption in liquid nitrogen. Ultraviolet-visible diffuse reflectance spectra (UV–Vis DRS) were obtained using a Cary 500 Scan UV–Vis Spectrophotometers, Varian, USA. X-ray photoelectron spectroscopy (XPS) measurement was carried out on a VG Scientific Microlab 310F system, using Mg Ka (1 253.6 eV) radiation as X-ray source. All the binding energies were referenced to the C1s peak at 285.0 eV with the surface adventitious carbon. The energy range for the whole spectrum is 0–800 eV, with 2 eV step length, which is 0.1 eV for the partial spectra. The sample has been sputtered by Ar with 3 kV voltage for 20 min to remove the surface pollution.

2.3 Photocatalytic activity of photocatalysts

Five hundred milliliters of phenol solution was loaded into a glass reactor stirred with a magnetic stirrer. The dosage of the photocatalysts is 0.5 g/L. First, the suspension was stirred for 30 min to adsorption balance, then a 1 000 W xenon lamp (with a 400 nm filter) was switched on to start the irradiation. The initial phenol concentration was about 17 mg/L. Ten milliliters samples were collected before and at regular intervals during the irradiation for analysis. The phenol concentration was determined by colorimetry at 510 nm after color reaction with 4-aminoantipyrine [10].

3 Results and discussion

3.1 Crystal structure of chlorine-doped TiO_2

Figure 1 shows the XRD patterns of chlorine-doped TiO_2 calcined at different temperatures. It can be seen from Fig. 1 that the chlorine-doped TiO_2 calcined at 210°C has already shown an anatase structure, and it is the mixture of anatase and amorphous. When calcined at 260°C the doped TiO_2 shows obviously anatase structure, and the crystallinity increases with the temperature. Previous researches have established that undoped TiO_2 calcined at 350°C were still present as amorphous [15], so the formation temperature for anatase phase should be above this temperature. Therefore, the incorporation of chlorine significantly decreases the transition temperature from amorphous to anatase. And this phenomenon may be also the result of strong acid treatment during the preparation. Rutile phase appears in the photocatalyst calcined at 300°C (Fig. 1), and its content increases with the temperature. The formation temperature of rutile phase is also much lower than the normal one in undoped TiO_2. Generally, rutile phase should be present over 600°C. Therefore, the induction of chlorine and acid treatment significantly decreases the phase transition temperature of chlorine-doped TiO_2.

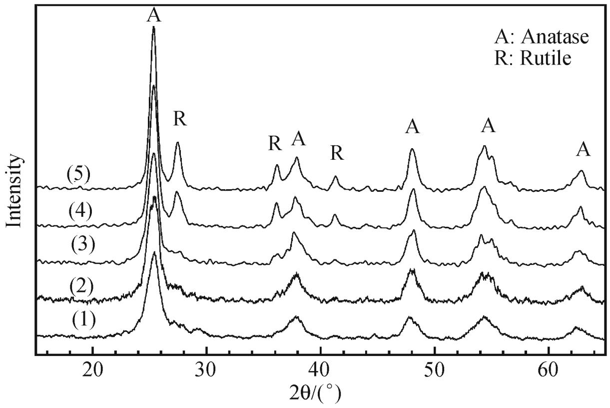

Fig. 1 X-ray diffraction (XRD) patterns of chlorine-doped TiO_2 calcined at different temperatures
(1) 210°C; (2) 260°C; (3) 300°C; (4) 350°C; (5) 400°C

Furthermore, the crystallite sizes of chlorine-doped TiO_2 can be calculated by Scherrer equation, shown in Eq. (1).

$$d = \frac{0.89\lambda}{\beta\cos\theta} \tag{1}$$

where d is the mean crystallite size, λ the wavelength of X-ray radiation used, 0.154 06 nm, β the line width at half-maximum height. The crystal lattice distortion (CLD) can be evaluated using the following equation

$$\varepsilon = \beta/4tg\theta \tag{2}$$

The weight of percentage of anatase in the samples can be calculated by the following equation

$$W_A = K_A A_A/(K_A A_A + A_R) \tag{3}$$

where A_A and A_R represent the intensity of the anatase peak at 101 and the rutile at 110 respectively, the constant K_A is 0.886 [16]. The calculated result of different samples is shown in Table 1. The mean crystallite sizes of these chlorine-doped TiO_2 became larger with increasing calcination temperature, while the values of CLD decreased. The reason for the decrease of CLD is that the degree of CLD is determined by chlorine content in the samples and oxygen may replace more chlorine with increasing calcination temperature, leading to the decrease of the CLD. On the other hand, the crystallinity can be improved by increasing the calcination temperature, also resulting to a decrease of CLD. The rutile phase appeared in the sample calcined at 300°C, and the content increased with the calcination temperature.

Table 1 Mean crystallite size, CLD, and phase constitutes of chlorine-doped TiO_2 calcined at different temperatures

Temperature /°C	210	260	300	350	400
β /(°)	1.017	0.899	0.806	0.733	0.502
Mean crystallite size /nm	7.93	8.97	10.00	11.0	16.1
CLD	1.14	1.00	0.899	0.818	0.560
Anatase percentage /%	100	100	96	77.5	73.9

Figure 2 shows the TEM photograph of chlorine-doped TiO_2 crystallite calcined at 300°C. It can be seen that doped TiO_2 nanoparticles are nearly spherical with an average size of about 10–20 nm. It is close to the results calculated by Scherrer equation. However, these nanoparticles aggregate to some extent and their size is not homogenous after agglomeration. The BET area of this sample is 158 m^2/g, even larger than the commercial Degussa P-25, indicating a good dispersibility of the doped TiO_2.

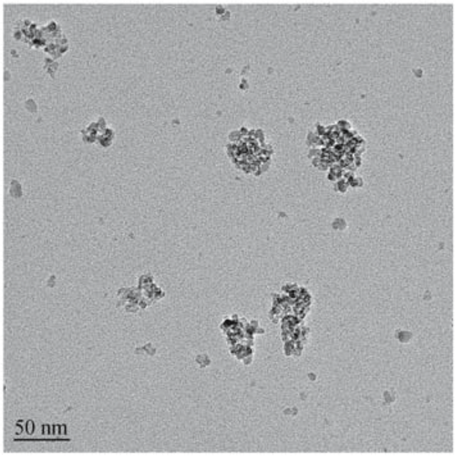

Fig. 2 TEM image of chlorine-doped TiO_2 nanoparticles calcined at 300°C

3.2 UV–Vis diffuse reflectance spectrum of chlorine-doped TiO_2

Figure 3 shows the DRS of the Degussa P-25 and the chlorine-doped TiO_2 calcined at 300°C. It can be found that the absorption onset of the Degussa P-25 (the undoped TiO_2) is lower than 400 nm, so its light response is restricted only in ultraviolet range. However, the chlorine-doped TiO_2 also shows strong absorbency in the visible range, and the absorption edge extends to nearly 700 nm. The change in the optical absorption property can be attributed to the presence of chlorine in TiO_2 crystal lattice. During the hydrolysis of tetra-butyl titanate in HCl, the chlorine migrated into the network of the formed gel, and replaced the oxygen in the TiO_2 crystal cell or existed in its interstitial void by heat treatment. Due to the presence of chlorine, some isolated levels between the valence band and conduction band may be formed, and photogenerated electrons and holes can transit through these intermediate levels. Therefore, the excitation energy for transition can be reduced to visible light range, and the chlorine-doped TiO_2 shows absorption in the visible light [17]. Due to the absorption changes, the chlorine-doped TiO_2 exhibits photocatalytic activity under visible light irradiation.

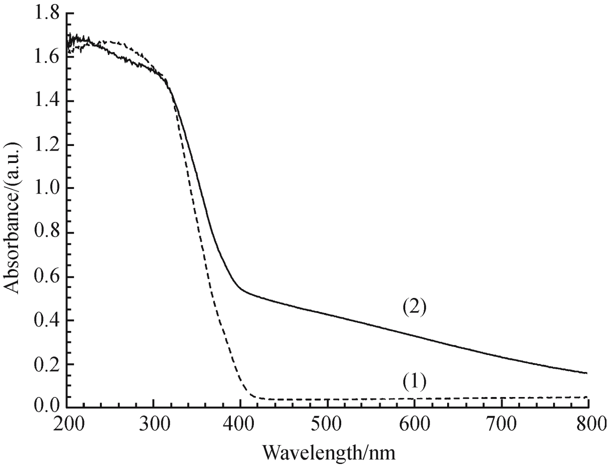

Fig. 3 UV-Vis diffuse reflection spectra of photocatalysts
(1) Degussa P-25; (2) chlorine-doped TiO_2

3.3 XPS of chlorine-doped TiO_2

The XPS is an important means to investigate the elementary components and their chemical states at the surface. To prove the presence of chlorine and identify its chemical state, the XPS of chlorine-doped TiO_2 calcined at 300°C was obtained and shown in Fig. 4. According to the peaks in the figure, Ti in the sample is present as Ti^{4+}, but the oxygen is present as complicated states. According to the O*1s* asymmetric peak, there are at least two kinds of oxygen species. They are crystal lattice oxygen (530.0 eV) and adsorbed oxygen, including chemically and physically adsorbed oxygen [18]. The chemical states of chlorine species are intricate. The highest peak of Cl $2p_3$ is 198.0 eV, which can be attributed to −1 valence chlorine. Under the calcination temperature, both HCl and $TiCl_4$ cannot exist in the sample, so chlorine must enter into the crystal lattice and replace oxygen, and exist as anion species. However, there are some other weak peaks at the higher binding energy. They may come from some adsorption species, or the interstitial chlorine in the crystal cell. The presence of chlorine can provide electrons for the band structure, form new levels in the band gap and induce a visible optical response property.

3.4 Photocatalytic activity of chlorine-doped TiO_2 under visible light irradiation

Because phenol is a typical recalcitrant contaminant without the sensitizing effect of dyes, it has been chosen as model pollutant to evaluate the photocatalytic activity of the samples

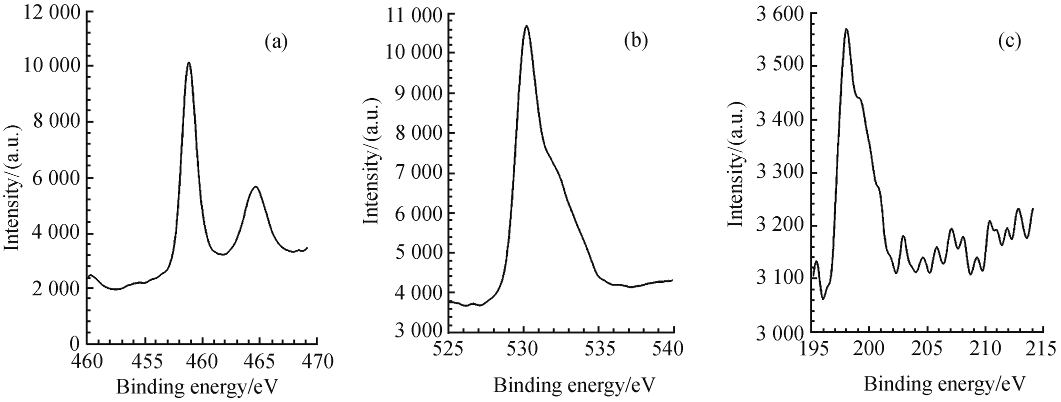

Fig. 4 XPS spectra of surface elements of chlorine-doped TiO_2 calcined at 300°C
(a) Ti 2*p*; (b) O 1*s*; (c) Cl 2*p*

[19]. Figure 5 shows the photocatalytic degradation curves of phenol on different samples. It can be found that in the dark the removal of phenol in 180 min is only 2.7% on the chlorine doped TiO_2 calcined at 300°C. However, under visible light irradiation, this sample demonstrates the highest activity, and the phenol concentration reduces as much as 42.5% in 120 min, even better than the nitrogen doped TiO_2 prepared by using similar methods [15].

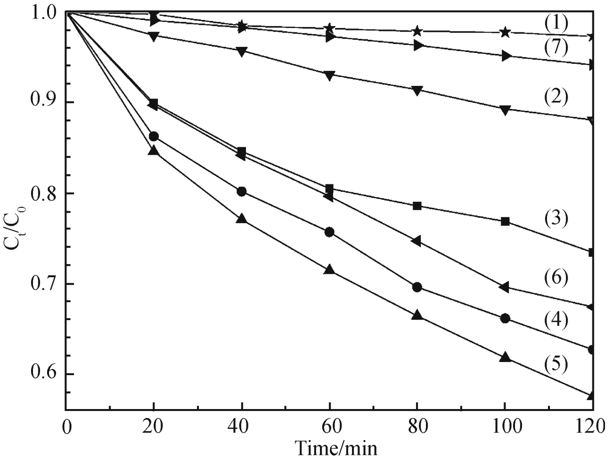

Fig. 5 Photocatalytic degradation of phenol in the presence of chlorine-doped TiO_2 calcined at different temperatures under visible light irradiation
(1) in dark; (2) Degussa P-25; (3) 210°C; (4) 260°C; (5) 300°C; (6) 350°C; (7) 400°C

Except the one calcined at 400°C, all chlorine-doped TiO_2 samples have better activity than the commercial Degussa P-25 under visible light irradiation. With the temperature increasing from 210°C to 300°C, chlorine-doped TiO_2 transformed from amorphous with low activity to high activity anatase structure, accompanied by an increase in crystallinity. All of these were favorable for improving photocatalytic performance. There was some rutile present in the sample calcined at 300°C. It has been reported that the mixture of rutile and anatase is favorable for the migration of photogenerated carriers [20], and always exhibits better activity than single anatase. Therefore, this sample shows the best photocatalytic activity. However, with further increase in calcination temperature, because the samples were calcined in air, the chlorine in the precursor would be replaced by oxygen and left gradually. And with the content of chlorine decreasing, the absorption in visible range disappeared and the photocatalytic activity under visible light decreased.

4 Conclusions

A novel chlorine-doped titanium dioxide photocatalyst with visible light response was prepared. The presence of chlorine efficiently decreased the band gap of TiO_2, and extended the absorption spectrum. The doped TiO_2 exhibited strong absorption in visible light range. The crystallization temperatures of these chlorine-doped TiO_2 were decreased significantly. These photocatalysts showed better photocatalytic performance under visible light irradiation. The one calcined at 300°C displayed the best activity, and the degradation ratio of phenol was 42.5% after 120 min.

Acknowledgements We are thankful for financial support by the Specialized Research Fund for the Doctoral Program of Higher Education (SRFDP, 20050248015) from the Ministry of Education. We gratefully acknowledge the support for transmission electron microscopy (TEM) measurements by Ms. Ruibin Wang and Ms. Xinqiu Guo of the Instrumental Analysis Center of Shanghai Jiao Tong University.

References

1. Carey J H, Lawrence J, Tosine H M. Photodechlorination of PCB's in the presence of titanium dioxide in aqueous suspensions. Bull Environ Contam Toxicol, 1976, 16(6): 697–701
2. Ji H W, Ma W H, Huang Y P, Zhao J C, Wang Z P. Reviews on photocatalysis of TiO_2 activated under visible light. Chin Sci Bull, 2003, 48(21): 2199–2204 (in Chinese)

3. Asahi R, Morikawa T, Ohwaki T, Aoki K, Taga Y. Visible-light photocatalysis in nitrogen-doped titanium oxides. Science, 2001, 293(5528): 269–271
4. Tang Y C, Huang X H, Yu H Q, Hu C. Characterization and visible-light-activity of nitrogen-doped TiO_2 photocatalyst. Chin J Inorg Chim, 2005, 21(11): 1747–1751 (in Chinese)
5. Livraghi S, Paganini M C, Giamello E, Selloni A, Di Valentin C, Pacchioni G. Origin of photoactivity of nitrogen-doped titanium dioxide under visible light. J Am Chem Soc, 2006, 128(49): 15666–15671
6. Khan S U M, Al-Shahry M, Ingler W B. Efficient photochemical water splitting by a chemically modified n-TiO_2. Science, 2002, 297(5590): 2243–2245
7. Sakthivel S, Kisch H. Daylight photocatalysis by carbon-modified titanium dioxide. Angew Chem Int Ed, 2003, 42(40): 4908–4911
8. Ohno T, Akiyoshi M, Umebayashi T, Asai K, Mitsui T, Matsumura M. Preparation of S-doped TiO_2 photocatalysts and their photocatalytic activities under visible light. Appl Catal A-Gen, 2004, 265(1): 115–121
9. Umebayashi T, Yamaki T, Itoh H, Asai K. Band gap narrowing of titanium dioxide by sulfur doping. Appl Phys Lett, 2002, 81(3): 454–456
10. Hong X T, Wang Z P, Cai W M, Lu F, Zhang J, Yang Y Z, Ma N, Liu Y J. Visible-light-activated nanoparticle photocatalyst of iodine-doped titanium dioxide. Chem Mater, 2005, 17(6): 1548–1552
11. Liu G, Chen Z G, Dong C L, Zhao Y N, Li F, Lu G Q, Cheng H M. Visible light photocatalyst: Iodine-doped mesoporous titania with a bicrystalline framework. J Phys Chem B, 2006, 110(42): 20823–20828
12. Zhao W, Ma W H, Chen C C, Zhao J C, Shuai Z G. Efficient degradation of toxic organic pollutants with Ni_2O_3/TiO_2-xBx under visible irradiation. J Am Chem Soc, 2004, 126(15): 4782–4783
13. Liu H Y, Gao L. Codoped rutile TiO_2 as a new photocatalyst for visible light irradiation. Chem Lett, 2004, 33(6): 730
14. Hua N P, Wu Z Y, Du Y K, Zou Z G, Yang P. Titanium dioxide nanoparticles codoped with pt and n for photodegradation of Cl_3CCOOH. Acta Phys-Chim Sin, 2005, 21(10): 1081–1085 (in Chinese)
15. Wang Z P, Cai W M, Hong X T, Zhao X L, Xu F, Cai C G. Photocatalytic degradation of phenol in aqueous nitrogen-doped TiO_2 suspensions with various light sources. Appl Catal B-Environ, 2005, 57(3): 223–231
16. Yu J C, Zhang L Z, Yu J G. Direct sonochemical preparation and characterization of highly active mesoporous TiO_2 with a bicrystalline framework. Chem Mater, 2002, 14(11): 4647–4653
17. Long M C, Cai W M, Wang Z P, Liu G Z. Correlation of electronic structures and crystal structures with photocatalytic properties of undoped, N-doped and I-doped TiO_2. Chem Phys Lett, 2006, 420(1–3): 71–76
18. Jing L Q, Li X Q, Li Z D, Wang B Q, Xin B F, Fu H G, Wang D J, Cai W M. XPS and SPS studies on nanometer Au/TiO_2 photocatalyst. Chin J Cata, 2005, 26(3): 189–193 (in Chinese)
19. Zhang F L, Zhao J C, Shen T, Hidaka H, Pelizzetti E, Serpone N. TiO_2-assisted photodegradation of dye pollutants—II. Adsorption and degradation kinetics of eosin in TiO_2 dispersions under visible light irradiation. Appl Catal B-Environ, 1998, 15(1–2): 147–156
20. Hurum D C, Agrios A G, Gray K A. Explaining the enhanced photocatalytic activity of degussa P25 mixed-phase TiO_2 using EPR. J Phys Chem B, 2003, 107(19): 4545–4549